Regulation of hepatic LDL receptors by mTORC1 and PCSK9 in mice

Ding Ai,[1] Chiyuan Chen,[2] Seongah Han,[1] Anjali Ganda,[1] Andrew J. Murphy,[1] Rebecca Haeusler,[1] Edward Thorp,[1] Domenico Accili,[1] Jay D. Horton,[2] and Alan R. Tall[1]

[1]Department of Medicine, Columbia University, New York, New York, USA. [2]Department of Molecular Genetics, University of Texas Southwestern Medical Center, Dallas, Texas, USA.

Individuals with type 2 diabetes have an increased risk of atherosclerosis. One factor underlying this is dyslipidemia, which in hyperinsulinemic subjects with early type 2 diabetes is typically characterized by increased VLDL secretion but normal LDL cholesterol levels, possibly reflecting enhanced catabolism of LDL via hepatic LDLRs. Recent studies have also suggested that hepatic insulin signaling sustains LDLR levels. We therefore sought to elucidate the mechanisms linking hepatic insulin signaling to regulation of LDLR levels. In WT mice, insulin receptor knockdown by shRNA resulted in decreased hepatic mTORC1 signaling and LDLR protein levels. It also led to increased expression of PCSK9, a known post-transcriptional regulator of LDLR expression. Administration of the mTORC1 inhibitor rapamycin caused increased expression of PCSK9, decreased levels of hepatic LDLR protein, and increased levels of VLDL/LDL cholesterol in WT but not *Pcsk9*$^{-/-}$ mice. Conversely, mice with increased hepatic mTORC1 activity exhibited decreased expression of PCSK9 and increased levels of hepatic LDLR protein levels. *Pcsk9* is regulated by the transcription factor HNF1α, and our further detailed analyses suggest that increased mTORC1 activity leads to activation of PKCδ, reduced activity of HNF4α and HNF1α, decreased PCSK9 expression, and ultimately increased hepatic LDLR protein levels, which result in decreased circulating LDL levels. We therefore suggest that PCSK9 inhibition could be an effective way to reduce the adverse side effect of increased LDL levels that is observed in transplant patients taking rapamycin as immunosuppressive therapy.

Introduction

Dyslipidemia is an important factor underlying the increased atherosclerosis risk of diabetic patients and is typically characterized by increased VLDL and reduced HDL, but surprisingly no change in LDL cholesterol levels (1). Metabolic studies have shown that increased hepatic VLDL lipid and apoB secretion are characteristics of type 2 diabetes and metabolic syndrome (2, 3), but that LDL fractional catabolism is increased at least in early type 2 diabetes when subjects are hyperinsulinemic (4). There was a strong correlation between hyperinsulinemia and the fractional catabolic rate (FCR) of LDL particles. Only in advanced diabetes, when plasma insulin levels were reduced, did LDL FCRs decrease (4). Since LDL catabolism is primarily mediated through the hepatic LDL receptor (LDLR) (5), this suggests that in early diabetes and metabolic syndrome hyperinsulinemia is associated with upregulation of hepatic LDLR, compensating for increased VLDL secretion and leading to no overall change in LDL levels.

Studies in cell culture and animal models have also linked insulin signaling to upregulation of LDLR (6, 7). Early studies in fibroblasts showed that insulin treatment increased LDLR numbers independent of cell proliferation (8). Regulation of the LDLR by insulin in HepG2 cells is PI3K dependent (9), but relevant pathways downstream of PI3K such as mTOR, FoxOs, or GSK3 (10) have not been elucidated. Decreased hepatic LDLR protein was clearly seen in LIRKO (liver-specific insulin receptor knockout) mice (11) and in mice with insulin receptor (*InsR*) knockdown (12). Based on these findings, we suggested that genetically restricted hepatic insulin signaling leads both to reduced VLDL lipid secretion and to decreased levels of hepatic LDLR (12). However, the mechanisms linking chronic changes in hepatic InsR to LDLR levels have not been elucidated.

Results

InsR knockdown suppresses hepatic LDLR expression via PCSK9. Knockdown of the hepatic InsR by shRNA in chow-fed, 5-hour-fasted C57BL/6 mice resulted in an 85% reduction in InsR and a 57% reduction in LDLR protein levels compared with controls (Figure 1A), as described previously (12), as well as decreased mTOR activity as shown by reduced phosphorylation of p70 ribosomal protein S6 kinase at T389 (p-S6K^{T389}) (Supplemental Figure 1A; supplemental material available online with this article; doi:10.1172/JCI61919DS1). However, there was no change in *Ldlr* mRNA levels, suggesting that the change in LDLR protein was due to a post-transcriptional regulatory event. Plasma insulin levels were reduced in *InsR* knockdown mice, but plasma glucose levels were unchanged (Supplemental Figure 1B). The mRNA levels of *Srebp-1c* and its target genes fatty acid synthase (*FAS*) and stearoyl-CoA desaturase–1 (*Scd1*) were decreased (Figure 1B), but expression of *Srebp-2* mRNA and its targets HMGCoA reductase (*HMGCoRed*) and HMGCoA synthase (*HMGCoSyn*) were unchanged, consistent with the lack of change in *Ldlr* mRNA. The post-transcriptional regulation of the LDLR may be mediated by proprotein convertase subtilisin/kexin type 9 (PCSK9) (13, 14) or LXR/inducible degrader of LDLR (IDOL) signaling pathways (15). Interestingly, in *InsR* knockdown mice *Pcsk9* mRNA and protein levels were increased 2- and 2.4-fold, respectively (Figure 1, A and B), while *Mylip* (encoding IDOL) mRNA was unchanged (Figure 1B). These findings suggested that increased PCSK9 might be responsible for the reduction in LDLR that results from decreased insulin signaling.

Conflict of interest: The authors have declared that no conflict of interest exists.
Citation for this article: *J Clin Invest.* 2012;122(4):1262–1270. doi:10.1172/JCI61919.

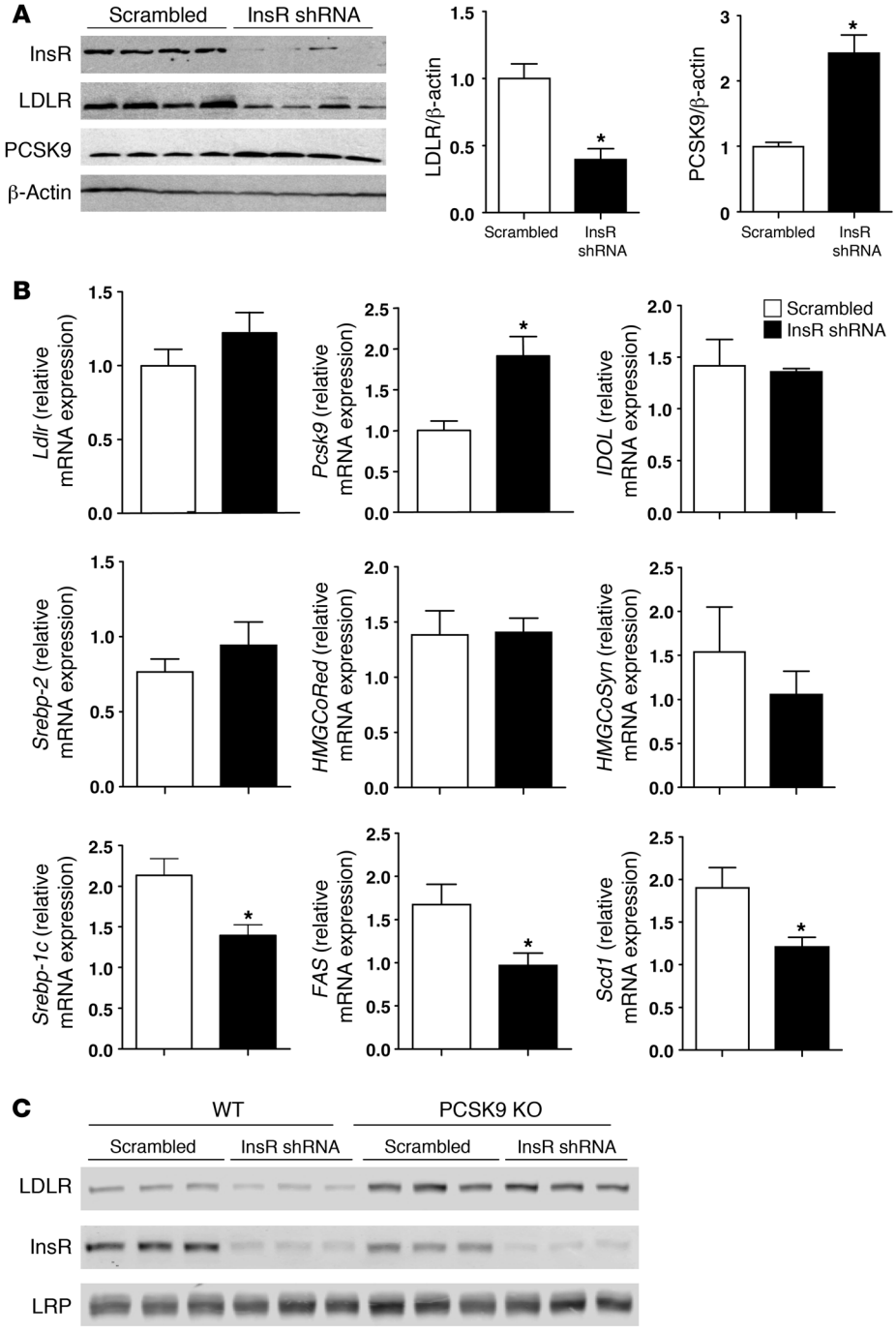

Figure 1
Effect of hepatic InsR knockdown in C57BL/6 mice. (**A**) Mice 10–11 weeks of age were injected with the InsR shRNA adenovirus and sacrificed on the 11th day after injection. Immunoblot analysis of InsR, LDLR, PCSK9, and β-actin in liver lysates from mice after infection with scrambled control adenovirus or InsR shRNA. Livers were collected after a 5-hour fast. Each lane shows the liver lysate of a different mouse. Right panel: Quantification of the Western blot results. (**B**) Analysis of hepatic gene expression by real-time qPCR in scrambled or InsR shRNA adenovirus–infected mice. (**C**) Membrane fraction of liver extract was prepared from *Pcsk9* knockout or WT mice after infection with scrambled control adenovirus or InsR shRNA and subjected to Western blot analysis of LDLR, InsR, and LRP. n = 4–5 mice per group. $^*P < 0.05$.

To further assess the significance of PCSK9 in the regulation of LDLR by insulin signaling, we treated WT or *Pcsk9*$^{-/-}$ mice with InsR shRNA. As expected (16), LDLR levels were higher in *Pcsk9*$^{-/-}$ mice (Figure 1C). Although the InsR was reduced by more than 80% in both strains and the LDLR was decreased by 59% in WT mice, there was no change in LDLR levels in *Pcsk9*$^{-/-}$ mice (Figure 1C). There was no change in *Ldlr* or *Mylip* mRNA among the groups (Supplemental Figure 1C). We also employed a genetic InsR knockdown model, *L1*^{B6}*Ldlr*$^{-/-}$ mice (12). In *L1*^{B6}*Ldlr*$^{-/-}$ mice, InsR knockdown resulted in decreased mTOR activity (p-S6K^{T389}) and increased Pcsk9 expression (Supplemental Figure 1, D and E). These data show that PCSK9 mediates the decrease in LDLR protein caused by reduced insulin signaling.

LDLR is regulated downstream of AKT independent of FoxO1 or GSK3β signaling. To further evaluate the role of the insulin signaling pathways in the regulation of LDLR, we injected adenovirus expressing constitutively active myristoylated AKT (myrAKT) or control adenovirus into the tail vein of C57BL/6 mice (Supplemental Figure 2A). This resulted in a decrease in *Pcsk9* expression and an increase in LDLR protein (Supplemental Figure 2, A and B). There were no significant changes in mRNA of *Srebp2* or its target genes including *Ldlr* (Supplemental Figure 2, A and B). We also evaluated

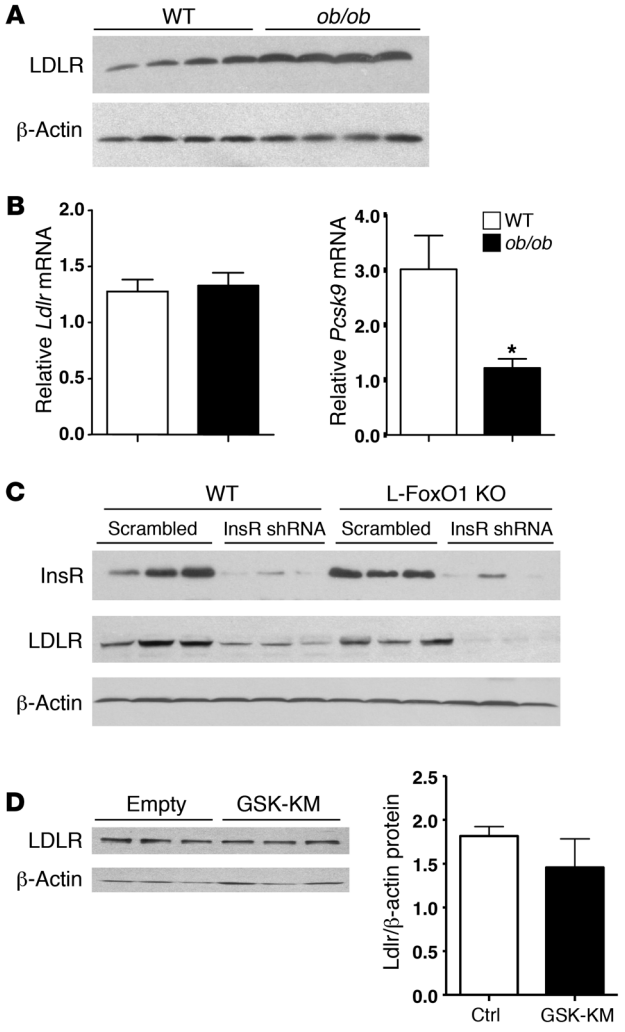

Figure 2
LDLR expression in *ob/ob* mice and the effect of AKT downstream effectors FoxO1 and GSK3β on LDLR expression. (**A**) The *ob/ob* mice and the control mice were 10–11 weeks of age. Liver were collected after a 5-hour fast. Immunoblot analysis of LDLR and β-actin is shown. (**B**) mRNA levels of *Ldlr* and *Pcsk9* in the mice. (**C**) Liver-specific FoxO1 knockout mice at 10–11 weeks of age were injected with the InsR shRNA adenovirus and sacrificed on the 11th day after injection. Immunoblot analysis of InsR, LDLR, and β-actin in liver lysates from mice after infection with scrambled control adenovirus or InsR shRNA. Livers were collected after a 5-hour fast. (**D**) LDLR expression in mice injected with dominant negative form of GSK3β-GSK-KM adenovirus. $n = 5$ mice per group. $^*P < 0.05$. Ctrl, control.

a possible role of PCSK9 in regulation of hepatic LDLR in *ob/ob* mice, in which we previously described increased levels of hepatic LDLR (12). LDLR protein levels were increased in livers of *ob/ob* mice, but there was no significant change in *Ldlr* mRNA levels (Figure 2, A and B). *Pcsk9* levels were decreased by 60% in livers of *ob/ob* mice (Figure 2B). Thus, *ob/ob* mice that were hyperinsulinemic and showed increased AKT phosphorylation in the fasting state and increased lipogenic gene expression had a phenotype opposite to that in mice in which insulin signaling is restricted by *InsR* knockdown, i.e., decreased *Pcsk9* and increased LDLR (17).

We next considered the potential involvement of each of the 3 major signaling pathways acting downstream of AKT: mTORC1, FoxO1, and GSK3β (10). AKT phosphorylates and leads to nuclear exclusion and inactivation of FoxO1; thus, if decreased insulin signaling by InsR shRNA and activation of FoxO1 were to mediate decreased LDLR expression, the reduction of LDLR by *InsR* knockdown should be abolished in liver-specific *FoxO1* knockout mice (L-FoxO1 KO) (18). In these mice we found that basal LDLR levels were unchanged, and following *InsR* knockdown LDLR levels were even more markedly reduced (Figure 2C) than in control mice. There were no changes in *Srebp-1c*, *Srebp-2*, *FAS*, *Scd1*, *HMGCoRed*, *HMGCoSyn*, *Ldlr*, *Pcsk9*, or *IDOL* mRNA levels in control compared with L-FoxO1 mice (Supplemental Figure 2C). AKT signaling also leads to phosphorylation and inactivation of GSK3β (10). Thus, if this pathway was involved, a dominant negative form of GSK3β should mimic the effect of AKT and lead to increased LDLR expression. We thus used an adenoviral vector expressing a dominant negative form of GSK3β (GSK-KM) in C57BL/6 mice but did not see an increase in LDLR expression (Figure 2D). There were no changes in *Srebp-1c*, *Srebp-2*, *FAS*, *Scd1*, *HMGCoRed*, *HMGCoSyn*, *Ldlr*, *Pcsk9*, or *IDOL* mRNA levels between control and GSK-KM mice (Supplemental Figure 2D). These data suggest that hepatic FoxO1 and GSK3β signaling pathways are not directly involved in the regulation of Pcsk9 and LDLR.

Hepatic mTORC1 regulates LDLR levels. After excluding the other two pathways, we determined whether activation of mTORC1 by AKT could change LDLR levels. To this end, we administered the mTOR inhibitor rapamycin (2 mg/kg/d) to C57BL/6 mice for 1 week. Phosphorylation of p70 ribosomal protein S6 kinase (p70s6k) was blocked by this treatment (Figure 3A), indicating effective inhibition of mTOR signaling. Rapamycin caused a reduction in LDLR protein levels and an increase in plasma cholesterol levels (Figure 3, A and B), whereas there was no significant change in the mRNA levels of *Ldlr*, *Srebp-2*, or its target genes (Supplemental Figure 3A). However, there was an increase in the mRNA and protein levels of PCSK9. There was no difference between rapamycin-treated and control mice in the mRNA levels of *Srebp-1c* and its target genes (Supplemental Figure 3A). These findings suggest that regulation of PCSK9 and LDLR by insulin signaling occurs via the mTORC1 pathway. To further assess the role of mTORC1 in the regulation of PCSK9 and LDLR, we treated WT and *Pcsk9* knockout mice with rapamycin or vehicle. The ability of rapamycin to reduce LDLR levels was abolished in *Pcsk9*$^{-/-}$ mice (Figure 3C). Moreover, while rapamycin caused an increase in VLDL/LDL cholesterol in WT mice, it had no effect on VLDL/LDL cholesterol in *Pcsk9*$^{-/-}$ mice (Figure 3D). Total cholesterol was increased in WT and *Pcsk9*$^{-/-}$ mice treated with rapamycin (Figure 3D), reflecting an increase in HDL caused by rapamycin treatment (data not shown). This indicates that the ability of rapamycin to decrease LDLR and increase VLDL/LDL cholesterol levels requires the presence of PCSK9.

To determine whether increased mTORC1 activity would be associated with reduced PCSK9 expression and increased levels of hepatic LDLR, as predicted by our model, we used mice with genetically increased mTORC1 activity, involving liver-specific knockout of the upstream inhibitor TSC1, i.e., *Li-Tsc1*$^{-/-}$ mice (19). These mice displayed an increase in hepatic mTORC1 activity (Figure 3E). Hepatic LDLR protein levels were increased 1.6-fold in *Li-Tsc1*$^{-/-}$ mice, *Ldlr* mRNA levels were unchanged, while *Pcsk9* mRNA levels were reduced by 48% in *Li-Tsc1*$^{-/-}$ mice (Figure 3, E and F).

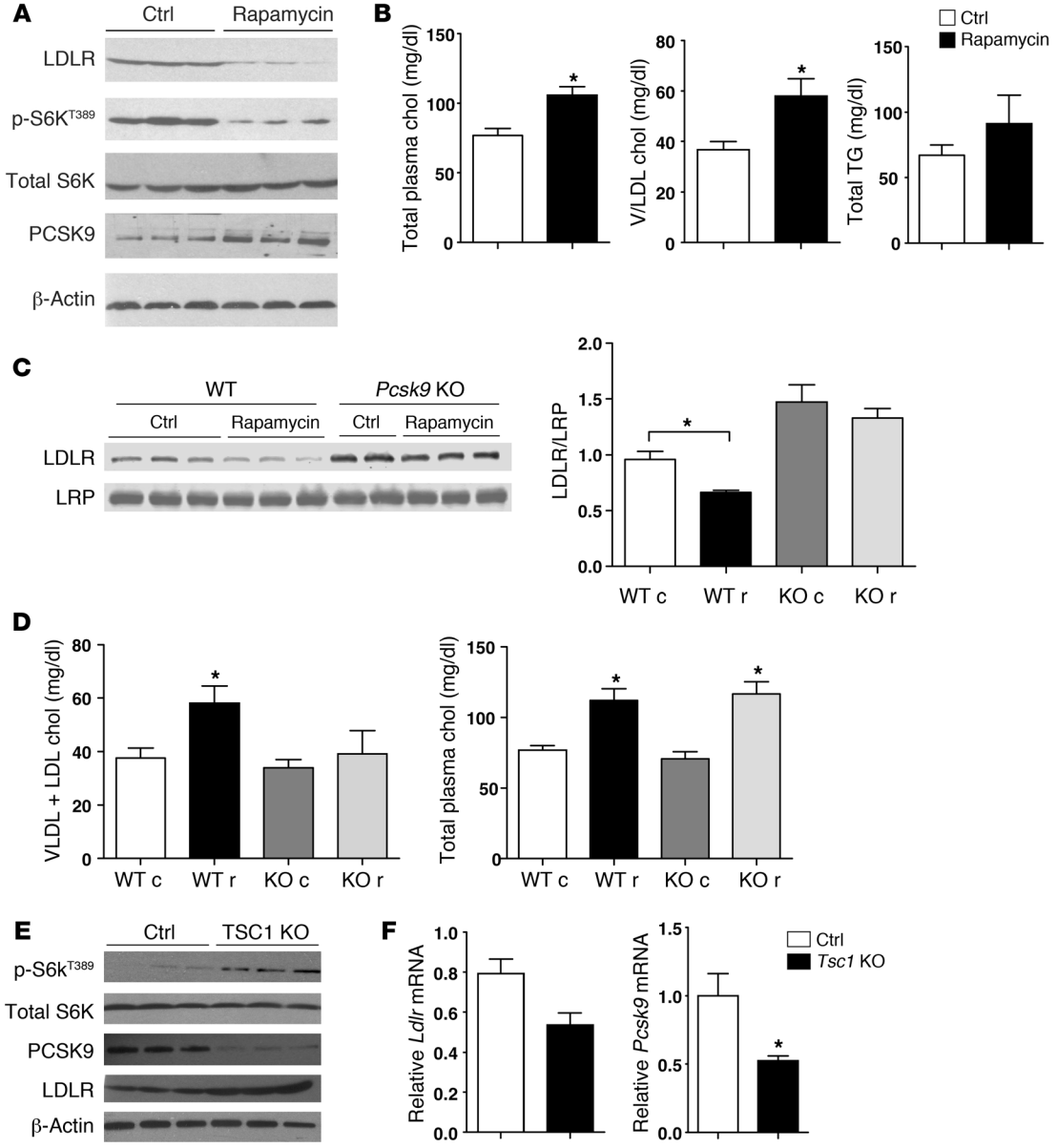

Figure 3

Effect of the mTOR inhibitor rapamycin on LDLR expression. (**A**) Immunoblot analysis of LDLR, p-S6K^{T389}, total S6K, PCSK9, and β-actin in mice treated with rapamycin. C57BL/6 mice fed a chow diet received saline/DMSO with or without rapamycin (2 mg/kg body weight) for 1 week. (**B**) Plasma total cholesterol (chol), VLDL plus LDL cholesterol, and triglyceride (TG) levels from **A** were measured. (**C**) Immunoblot analysis of LDLR and LRP in the membrane fraction of the liver of the mice treated with rapamycin. C57BL/6 or *Pcsk9*$^{-/-}$ mice fed a chow diet received saline/DMSO (control [c]) with or without rapamycin (r; 2 mg/kg body weight) for 1 week. $n = 5$. Right panel: Quantification of the Western blot results; $^*P < 0.05$. (**D**) Plasma VLDL plus LDL cholesterol and total cholesterol were measured in the mice described in **C**. (**E**) Immunoblot analysis of LDLR, p-S6 kinase^{T389}, total S6K, PCSK9, and β-actin. (**F**) Hepatic mRNA levels of *Ldlr* and *Pcsk9* in the mice. $n = 5$–6 mice per group. $^*P < 0.05$.

mTORC1 induces transcription of PCSK9 in an HNF1α-dependent manner. We carried out further studies to explore potential mechanisms underlying the mTORC1-mediated increase in *Pcsk*9 mRNA levels. Recently, HNF1α was shown to mediate the transcriptional induction of *Pcsk9* (20, 21) via a highly conserved *cis*-acting element 28 bp upstream of the sterol regulatory element (SRE) in the *Pcsk9* promoter (20, 21). Consistent with a role of HNF1α in the induction of PCSK9 in the two mouse models with decreased hepatic mTORC1 activity, the protein level of HNF1α was increased in both *InsR* knockdown and rapamycin-treated mice (Figure 4, A and B), while the cognate mRNA levels were increased 2.5-fold and 2.4-fold (Figure 4, A and B). Furthermore, ChIP analysis showed increased occupancy by HNF1α of its binding site in the *Pcsk9* promoter region, which included the identified HNF1α binding site (20) (proximal) rather than a control region that is 903 bp from the binding site (distal), following rapamycin treatment (Figure

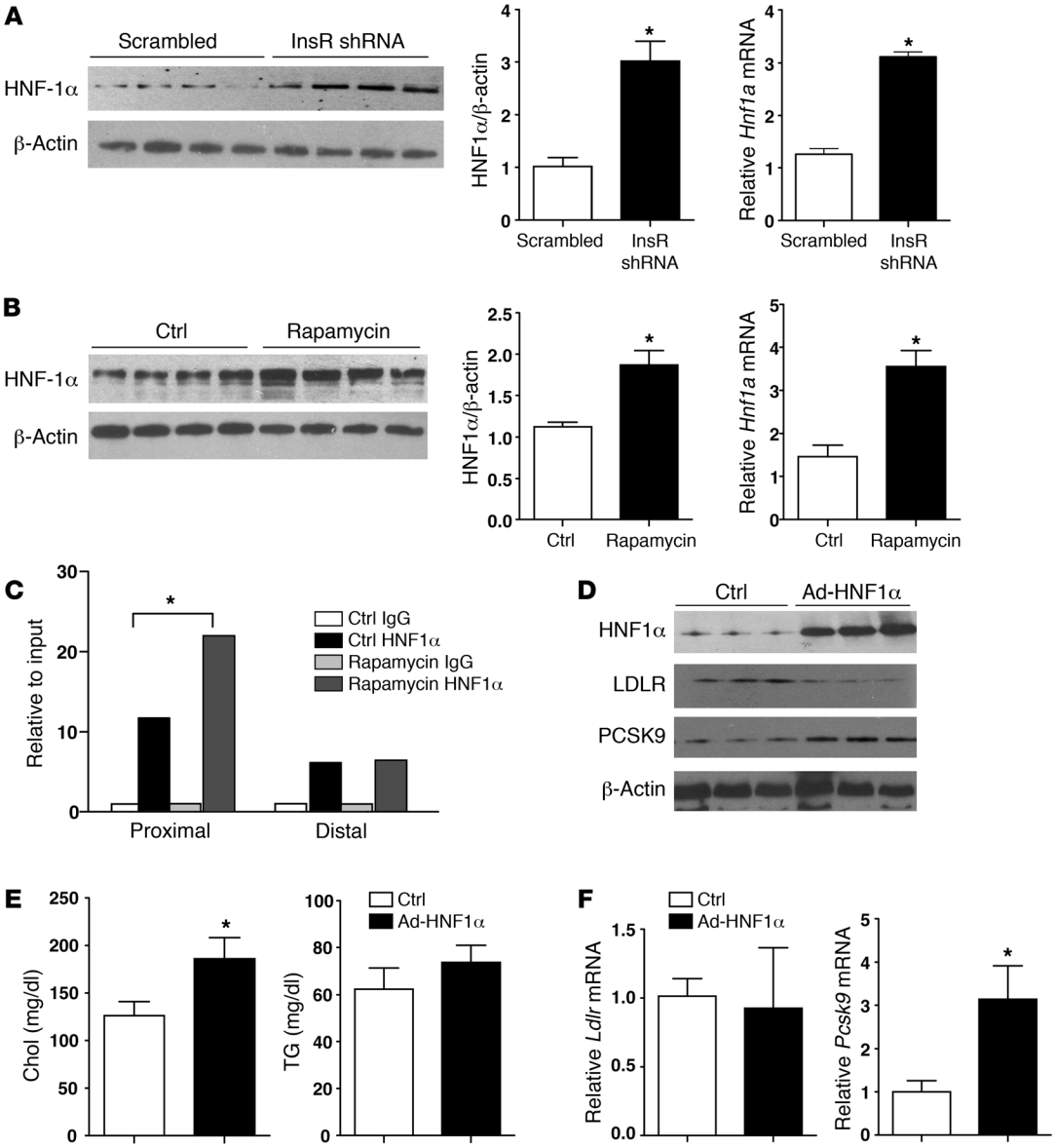

Figure 4

HNF1α is involved in the regulation of LDLR by insulin signaling. (**A** and **B**) Immunoblot and real-time qPCR analysis of HNF1α in InsR- or scrambled shRNA–injected mice and vehicle- or rapamycin-treated mice. (**C**) *Pcsk*9 promoter ChIP assay in the liver of vehicle- or rapamycin-treated mice using the HNF1α or IgG antibody. (**D**) *ob/ob* mice were killed 4 days after HNF1α adenovirus (Ad-HNF1α) injection and following a 6-hour fast. Immunoblot analysis of the HNF1α, LDLR, PCSK9, and β-actin. (**E**) Plasma cholesterol and triglyceride concentrations. (**F**) Hepatic mRNA levels of *Ldlr* and *Pcsk9* in the mice. $n = 5$ mice/group. $^*P < 0.05$.

4C). Also consistent with a role of altered HNF1α expression in the regulation of *Pcsk9*, we found reduced hepatic expression of HNF1α in *ob/ob* mice (Supplemental Figure 4A) and *Li-Tsc1*$^{-/-}$ mice (Supplemental Figure 3B), and the binding of HNF1α to the *Pcsk9* promoter was decreased in *Li-Tsc1*$^{-/-}$ mice (Supplemental Figure 3C). Furthermore, adenoviral overexpression of HNF1α in livers of *ob/ob* mice led to increased mRNA and protein levels of PCSK9, decreased LDLR protein but not mRNA levels (Figure 4, D and F), and increased plasma cholesterol levels (Figure 4E), while there were no changes in the expression of hepatic *Srebp-1c*, *Srebp-2*, or their target genes (Supplemental Figure 4B).

mTOR has been shown to activate PKCδ (22, 23), and PKCδ has been reported to play an important role in hepatic insulin resistance, glucose intolerance, and hepatosteatosis in obese humans and mice (24). Consistent with a role of mTORC1 in its activation, *Li-Tsc1*$^{-/-}$ mice exhibited markedly enhanced serine 662 phosphorylation of hepatic PKCδ. Since activated PKCs can induce nuclear exclusion of HNF4α (25) and HNF4α activates HNF1α (26), we evaluated the nuclear levels of HNF4α in *Li-Tsc1*$^{-/-}$ mice. Consistent with a role of HNF4α upstream of HNF1α, nuclear HNF4α was decreased by 51% (Figure 5A) and total HNF1α by 44% compared with control mice (Figure 5A). To more directly assess the role of

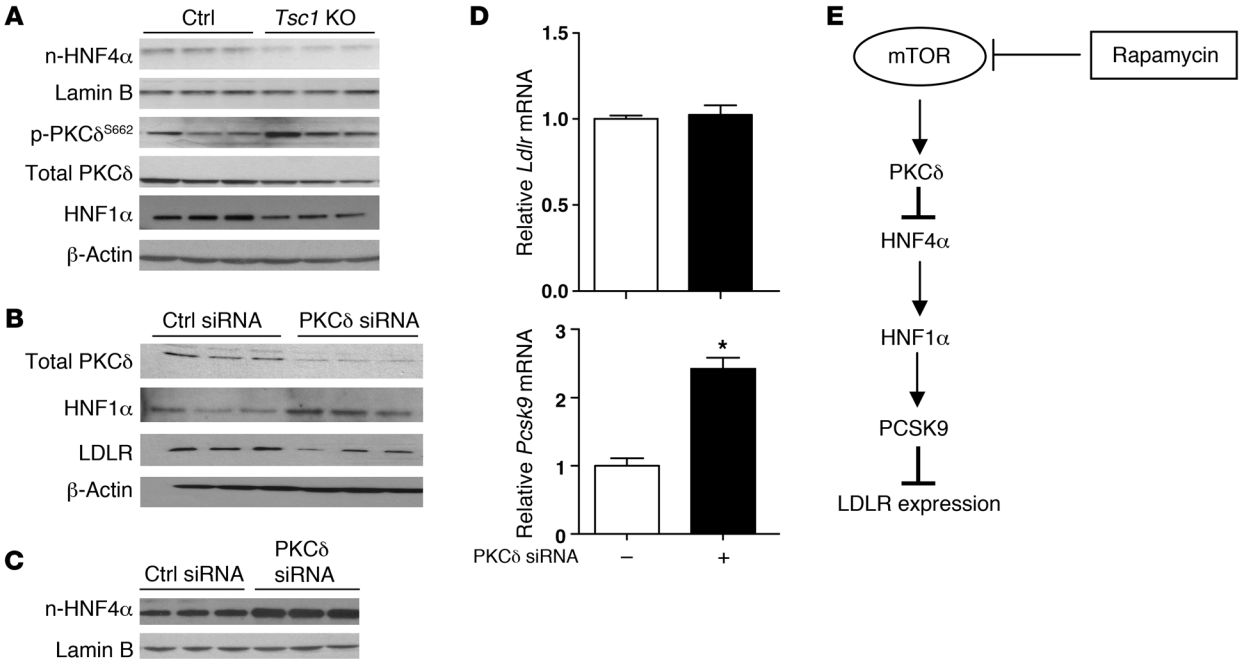

Figure 5
The potential mechanism of the regulation of LDLR by mTOR (**A**) Immunoblot analysis of PKCδ-pS^{662} and total-PKCδ from liver lysate. Nuclear HNF4α (n-HNF4α) and lamin B were measured by Western blot in liver nuclear extracts. $n = 4$. (**B**) Immunoblot analysis of total PKCδ, HNF1α, LDLR, and β-actin in *Tsc1*-null MEFs harvested at 24 hours after transfection with control or PKCδ siRNA. (**C**) Immunoblot analysis of nuclear-HNF4α and lamin B in nuclear extracts from *Tsc1*-null MEFs transfected with control or PKCδ siRNA. (**D**) mRNA levels of *Pcsk9* and *Ldlr* in *Tsc1*-null MEFs transfected with control or PKCδ siRNA were measured. $n = 3$; $^*P < 0.05$. (**E**) A proposed model for the regulation of LDLR by insulin signaling.

PKCδ in the regulation of PCSK9 and LDLR, we transfected *Tsc1*-null mouse embryonic fibroblasts (MEFs), which have increased mTORC1 activity (27), with control or PKCδ siRNA. Total HNF1α and nuclear HNF4α were both increased following PKCδ knockdown; *Pcsk9* mRNA was increased; and protein but not mRNA levels of *Ldlr* were decreased in response to PKCδ knockdown in the *Tsc1*$^{-/-}$ MEFs (Figure 5, B–D). Furthermore, ChIP analysis showed increased occupancy by HNF1α of its binding site in the *Pcsk9* promoter region, which includes the identified HNF1α binding site (20) (proximal) rather than the region that is 903 bp from the binding site (distal), following PKCδ knockdown in *Tsc1*$^{-/-}$ MEFs (Supplemental Figure 5). These findings are consistent with the model shown in Figure 5E, in which PCKδ activation downstream of increased mTORC1 activity leads to repression of HNF4α/1α, reduced PCSK9, and increased LDLR.

Discussion

In hyperinsulinemic obese mouse models, the liver is insulin resistant in terms of gluconeogenesis but remains insulin sensitive for lipogenesis (17), VLDL secretion, and LDLR expression (11, 12). Insulin signaling via AKT2 and mTORC1 has emerged as having a key role in the regulation of hepatic lipogenesis in obese mice (28, 29), likely with involvement of additional pathways/effects downstream of AKT (30, 31). Interestingly, our studies also implicate AKT/mTORC1 signaling in the regulation of hepatic LDLRs. The underlying mechanism involves induction of PCSK9 via mTORC1, leading to post-transcriptional downregulation of hepatic LDLR. The relationship between mTORC1 activity and regulation of LDLR via PCSK9 was demonstrated in two mouse models with reduced hepatic mTORC1 activity, rapamycin- and InsR shRNA–treated mice, and in two models with increased mTORC1 activity, *ob/ob* and *Li-Tsc1*$^{-/-}$ mice. We provide evidence for involvement of PCSK9 in the first two models by demonstrating that the effects of rapamycin or InsR knockdown on LDLR were abolished in *Pcsk9*$^{-/-}$ mice. Consistent with recent evidence (21), our data suggest that HNF1α is responsible for the transcriptional regulation of *Pcsk9* gene expression in these models, with increased HNF1α levels shown in rapamycin- and InsR shRNA–treated mice and reduction in LDLR levels in *ob/ob* mice by HNF1α overexpression. Further analysis of potential signaling pathways in *Li-Tsc1*$^{-/-}$ mice and fibroblasts suggested activation of PKCδ downstream of mTORC1, leading to nuclear exclusion of HNF4α, decreased HNF1α, and decreased *Pcsk9* expression (Figure 5E). Interestingly, PKCδ is induced by a high-fat diet in C57BL/6 mice, with adverse effects on hepatic lipogenesis and gluconeogenesis, possibly mediated through effects on p70 S6K, a known mTORC1 effector (24). mTORC1 represents a central hub integrating information not only from insulin signaling but also from nutritional stimuli and cytokines (32). Thus, it is likely that the prominent induction of LDLR in obese mice reflects multiple chronic inputs to mTORC1 in addition to effects of insulin/AKT signaling.

PCSK9 is a member of the mammalian subtilisin family of proprotein convertases (33) that regulates circulating LDL cholesterol levels primarily by diverting recycling LDLRs into the endosomal-lysosomal pathway, leading to LDLR degradation. PCSK9 was also identified as a SREBP-2– and dietary cholesterol–regu-

lated gene in livers of mice (34, 35). Humans with loss-of-function mutations (36) and *Pcsk9* knockout mice have significantly reduced circulating LDL cholesterol levels, reflecting increased LDLR protein levels (16, 36). Loss-of-function mutations in *Pcsk9* are also associated with a marked reduction in cardiovascular disease (13, 37). Several different approaches to inhibit PCSK9 function for the treatment of hypercholesterolemia have been undertaken. PCSK9 antisense oligonucleotides administered to mice increased hepatic LDLR expression and lowered plasma cholesterol (38). Administration of RNAi against PCSK9 delivered using lipidoid nanoparticles to cynomolgus monkeys reduced plasma LDL cholesterol by approximately 60% (39). Antibody inhibition of PCSK9 in cynomolgus monkeys also reduced LDL cholesterol levels by as much as 80% (39, 40).

Previous studies in cultured cells have shown that rapamycin can reduce LDLR levels independent of changes in SREBP-2 expression (41–43), However, the in vivo significance and mechanism of this effect were unknown. Our studies suggest that the post-transcriptional downregulation of hepatic LDLR protein levels via PCSK9 is responsible for the increased LDL levels induced by rapamycin, implying that this adverse effect of rapamycin treatment could be overcome by therapeutic inhibition of PCSK9. As an mTORC1 inhibitor, rapamycin is a potent immunosuppressive agent used in transplantation medicine because of its low renal toxicity. However, a major side effect of rapamycin is hypercholesterolemia and increased LDL levels, likely contributing to cardiovascular disease, a leading cause of mortality after kidney transplantation (44). In addition, dyslipidemia has been implicated as a risk factor for chronic allograft loss (45). It is important to note that statin treatment upregulates transcription of both LDLR and its natural inhibitor PCSK9. Following depletion of the intracellular cholesterol pool, a processed mature form of SREBP-2 enters the nucleus, where it binds to the SRE of both the LDLR and PCSK9 promoters, activating transcription. The protein product of *PCSK9* gene transcription reduces LDLR protein levels, and this intrinsic regulatory loop has been recognized as an undesirable limitation of statin-related LDL cholesterol–lowering capacity (20). In a recent systematic review of randomized controlled trials that attempted to characterize mTOR inhibitor dyslipidemia in kidney transplant patients, approximately 60% of mTOR inhibitor–treated patients received lipid-lowering agents (2-fold greater than non-mTOR inhibitor–treated patients) (28). Given our finding that post-transcriptional downregulation of LDLR protein levels via PCSK9 is directly responsible for the increased circulating LDL induced by rapamycin, it follows that statin therapy, which affects LDLR at the transcriptional level and also increases PCSK9, would likely have limited efficacy. Paradoxically, Mueller et al. (46) reported that rapamycin induced hypercholesterolemia in *Ldlr*$^{-/-}$ mice but nevertheless caused a reduction in atherosclerosis. This along with our earlier study (12) indicates that rapamycin has an additional mechanism such as increased VLDL secretion that leads to increased VLDL cholesterol independent of LDLR, and implies a potent antiatherogenic effect of rapamycin independent of plasma lipids. In regard to possible antiatherogenic effects, a recent study suggested that inhibition of mTORC1 and consequent induction of autophagy would led to increased cholesterol efflux from macrophage foam cells (47). While the overall effects of rapamycin on atherogenesis in humans remains unknown, it seems likely that our studies are relevant to the mechanisms by which rapamycin raises LDL levels in humans and that this effect is likely pro-atherogenic. Our studies imply that therapeutic inhibition of PCSK9 might effectively treat hypercholesterolemia in transplant patients receiving rapamycin, and could potentially have a beneficial effect in cardiovascular disease, allograft loss, and mortality in this population.

Methods

Animals. C57BL/6, *L-FoxO1*, and *Pcsk9* knockout mice were killed using CO_2 11 days after tail injection of InsR shRNA or GSK-KM or myrAKT adenovirus or their control adenovirus and following a 5-hour fast. C57BL/6 mice or *Pcsk9* knockout mice received 400 μl PBS/0.1% DMSO supplemented with rapamycin (2 mg/kg body weight; LC Laboratories) through intraperitoneal injection every day. After 1-week injections, mice were anesthetized by CO_2, and blood and liver tissues were collected from non-fasted mice. Mice carrying a floxed allele of *Tsc1* (*Tsc1*$^{loxP/loxP}$) (48) were purchased from The Jackson Laboratory. Adenovirus expressing Cre (adenovirus-Cre; 5×10^{10} PFU/ml; 100 μl) or control adenovirus (adenovirus-empty) was administered via tail vein injection under isoflurane anesthesia to mice at 8 weeks in age, and the mice were killed on the seventh day after injection following a 5-hour fast. *ob/ob* mice, 8–10 weeks old, were killed using CO_2 4 days after mouse HNF1α or control adenovirus injection and following a 6-hour fast. Mice had free access to food and water and were housed in a pathogen-free facility according to animal welfare guidelines established by the Office of Laboratory Animal Welfare (OLAW) of the NIH. All experiments were reviewed and approved by the Columbia University Institutional Animal Care and Use Committee and were conducted according to that committee's guidelines.

Plasma triglyceride and cholesterol determination. Blood samples were collected by retroorbital venous plexus puncture. Plasma was separated by centrifugation and stored at –70°C until analysis. Total plasma cholesterol and triglycerides were measured with Wako enzymatic kits and Infinity (Thermo Scientific) according to the manufacturers' instructions.

Immunoblot analysis. Western blot analysis was carried out using the following primary antibodies: anti–p-AKT (Cell Signaling Technology); anti-InsR (Santa Cruz Biotechnology Inc.); anti–p-S6K^{T389} (Cell Signaling Technology); anti–S6K (Cell Signaling Technology), anti-HNF4α (R&D Systems), anti–lamin B (Abcam), anti-PKCδpS664 (Invitrogen), anti–total PKCδ (Santa Cruz Biotechnology Inc.), anti-HNF1α (Santa Cruz Biotechnology Inc.), anti–LDLR-related protein (anti-LRP) (14), anti-LDLR (Abcam); anti-PCSK9 (gift from Jan L. Breslow's laboratory, the Rockefeller University, New York, New York, USA) and anti–β-actin antibody (Sigma-Aldrich). Nuclear extract was isolated by NE-PER (Thermo), and liver lysate was prepared with T-PER (Thermo). Protein samples were separated by SDS-PAGE and transferred onto nitrocellulose membranes (Bio-Rad). Membranes were probed separately with antibodies as described in the respective figure legends. Following incubation with horseradish peroxidase–conjugated secondary antibodies, proteins were visualized with SuperSignal West Pico Chemiluminescent reagents (Pierce; Thermo Scientific) on x-ray films. The band intensity was quantified using scanning densitometry of the autoradiogram with NIH ImageJ software (http://rsb.info.nih.gov/ij/).

Real-time quantitative PCR analysis. Liver tissues were homogenized and total RNA was isolated using RNAzol B (Tel-Test) according to the manufacturer's instructions. Total RNA (2 μg) was reverse transcribed at 42°C with SuperScript II (Life Technologies). Gene expression was measured using SYBR Green PCR core reagents (Applied Biosystems). Transcript levels of β-actin were used for normalization across samples. The sequences of PCR probes and primers used are described in Supplemental Table 1.

ChIP assays. Chromatin lysates from mouse livers were cross-linked in 1% formaldehyde for 15 minutes, and then liver nuclei were isolated by NE-PER kit, followed by sonication. After being precleared with protein G agarose beads, chromatin lysates were immunoprecipitated using antibod-

ies against HNF1α (Santa Cruz Biotechnology Inc.) or control rabbit IgG in the presence of BSA and salmon sperm DNA. Beads were extensively washed before reverse cross-linking. Sample DNA was isolated from the immunoprecipitates and then amplified by quantitative PCR (qPCR) using primers flanking the enhancer (distal, 903 bp from the identified HNF1α binding site; ref. 20) or the proximal promoter (proximal, including the identified HNF1α binding site) regions (Supplemental Table 1).

siRNA transfection. *Tsc1*$^{-/-}$ MEFs were cultured as previously described (27). Mouse PKCδ and control siRNA were supplied by Ira Tabas (Columbia University Medical Center, New York, New York, USA). Lipofectamine RNAiMAX (Invitrogen) was used. Transfection was performed according to the manufacturer's instructions.

Statistics. Results are expressed as mean ± SEM (*n* is indicated in the figure legends or figures). Results were analyzed using a 2-tailed Student's *t* test or 1-way ANOVA where appropriate, using GraphPad Prism software. A *P* value less than 0.05 was considered statistically significant.

Study approval. All animal experiments were reviewed and approved by the Columbia University Institutional Animal Care and Use Committee and were conducted according to that committee's guidelines.

Acknowledgments

The authors thank Jan L. Breslow for providing antibody and the members of Domenico Accili's and Alan Tall's laboratories for support and discussion. We thank Aristotelis Astreinidis (Drexel University College of Medicine, Philadelphia, Pennsylvania, USA) for providing *Tsc1*$^{-/-}$ MEFs. This work is supported by NIH grants HL020948 (to C. Chen and J.D. Horton) and HL087123 (to D. Ai and A.R. Tall).

Received for publication November 11, 2011, and accepted in revised form February 1, 2012.

Address correspondence to: Ding Ai, Columbia University Medical Center, P&S8-401, 630 West 168th Street, New York, New York 10032, USA. Phone: 212.305.5789; Fax: 212.305.5052; E-mail: da2424@columbia.edu.

Seongah Han's present address is: Merck & Co. Inc., Whitehouse Station, New Jersey, USA.

1. Krauss RM. Lipids and lipoproteins in patients with type 2 diabetes. *Diabetes Care*. 2004;27(6):1496–1504.
2. Adiels M, et al. Overproduction of VLDL1 driven by hyperglycemia is a dominant feature of diabetic dyslipidemia. *Arterioscler Thromb Vasc Biol*. 2005; 25(8):1697–1703.
3. Myerson M, et al. Treatment with high-dose simvastatin reduces secretion of apolipoprotein B-lipoproteins in patients with diabetic dyslipidemia. *J Lipid Res*. 2005;46(12):2735–2744.
4. Kissebah AH, Alfarsi S, Evans DJ, Adams PW. Plasma low density lipoprotein transport kinetics in noninsulin-dependent diabetes mellitus. *J Clin Invest*. 1983;71(3):655–667.
5. Brown MS, Goldstein JL. A receptor-mediated pathway for cholesterol homeostasis. *Science*. 1986; 232(4746):34–47.
6. Streicher R, et al. SREBP-1 mediates activation of the low density lipoprotein receptor promoter by insulin and insulin-like growth factor-I. *J Biol Chem*. 1996; 271(12):7128–7133.
7. Sekar N, Veldhuis JD. Involvement of Sp1 and SREBP-1a in transcriptional activation of the LDL receptor gene by insulin and LH in cultured porcine granulosa-luteal cells. *Am J Physiol Endocrinol Metab*. 2004;287(1):E128–E135.
8. Chait A, Bierman EL, Albers JJ. Low-density lipoprotein receptor activity in cultured human skin fibroblasts. Mechanism of insulin-induced stimulation. *J Clin Invest*. 1979;64(5):1309–1319.
9. Borradaile NM, de Dreu LE, Huff MW. Inhibition of net HepG2 cell apolipoprotein B secretion by the citrus flavonoid naringenin involves activation of phosphatidylinositol 3-kinase, independent of insulin receptor substrate-1 phosphorylation. *Diabetes*. 2003;52(10):2554–2561.
10. Manning BD, Cantley LC. AKT/PKB signaling: navigating downstream. *Cell*. 2007;129(7):1261–1274.
11. Biddinger SB, et al. Hepatic insulin resistance is sufficient to produce dyslipidemia and susceptibility to atherosclerosis. *Cell Metab*. 2008;7(2):125–134.
12. Han S, et al. Hepatic insulin signaling regulates VLDL secretion and atherogenesis in mice. *J Clin Invest*. 2009;119(4):1029–1041.
13. Benjannet S, et al. NARC-1/PCSK9 and its natural mutants: zymogen cleavage and effects on the low density lipoprotein (LDL) receptor and LDL cholesterol. *J Biol Chem*. 2004;279(47):48865–48875.
14. Park SW, Moon YA, Horton JD. Post-transcriptional regulation of low density lipoprotein receptor protein by proprotein convertase subtilisin/kexin type 9a in mouse liver. *J Biol Chem*. 2004;279(48):50630–50638.
15. Zelcer N, Hong C, Boyadjian R, Tontonoz P. LXR regulates cholesterol uptake through Idol-dependent ubiquitination of the LDL receptor. *Science*. 2009;325(5936):100–104.
16. Rashid S, et al. Decreased plasma cholesterol and hypersensitivity to statins in mice lacking Pcsk9. *Proc Natl Acad Sci U S A*. 2005;102(15):5374–5379.
17. Shimomura I, Matsuda M, Hammer RE, Bashmakov Y, Brown MS, Goldstein JL. Decreased IRS-2 and increased SREBP-1c lead to mixed insulin resistance and sensitivity in livers of lipodystrophic and ob/ob mice. *Mol Cell*. 2000;6(1):77–86.
18. Matsumoto M, Pocai A, Rossetti L, Depinho RA, Accili D. Impaired regulation of hepatic glucose production in mice lacking the forkhead transcription factor Foxo1 in liver. *Cell Metab*. 2007;6(3):208–216.
19. Sengupta S, Peterson TR, Laplante M, Oh S, Sabatini DM. mTORC1 controls fasting-induced ketogenesis and its modulation by ageing. *Nature*. 2010;468(7327):1100–1104.
20. Dong B, et al. Strong induction of PCSK9 gene expression through HNF1alpha and SREBP2: mechanism for the resistance to LDL-cholesterol lowering effect of statins in dyslipidemic hamsters. *J Lipid Res*. 2010;51(6):1486–1495.
21. Li H, Dong B, Park SW, Lee HS, Chen W, Liu J. Hepatocyte nuclear factor 1alpha plays a critical role in PCSK9 gene transcription and regulation by the natural hypocholesterolemic compound berberine. *J Biol Chem*. 2009;284(42):28885–28895.
22. Rokaw MD, West M, Johnson JP. Rapamycin inhibits protein kinase C activity and stimulates Na+ transport in A6 cells. *J Biol Chem*. 1996;271(50):32468–32473.
23. Parekh D, Ziegler W, Yonezawa K, Hara K, Parker PJ. Mammalian TOR controls one of two kinase pathways acting upon nPKCdelta and nPKCepsilon. *J Biol Chem*. 1999;274(49):34758–34764.
24. Bezy O, et al. PKCdelta regulates hepatic insulin sensitivity and hepatosteatosis in mice and humans. *J Clin Invest*. 2011;121(6):2504–2517.
25. Sun K, et al. Phosphorylation of a conserved serine in the deoxyribonucleic acid binding domain of nuclear receptors alters intracellular localization. *Mol Endocrinol*. 2007;21(6):1297–1311.
26. Qadri I, Iwahashi M, Kullak-Ublick GA, Simon FR. Hepatocyte nuclear factor (HNF) 1 and HNF4 mediate hepatic multidrug resistance protein 2 up-regulation during hepatitis C virus gene expression. *Mol Pharmacol*. 2006;70(2):627–636.
27. Kwiatkowski DJ, et al. A mouse model of TSC1 reveals sex-dependent lethality from liver hemangiomas, and up-regulation of p70S6 kinase activity in Tsc1 null cells. *Hum Mol Genet*. 2002;11(5):525–534.
28. Kasiske BL, et al. Mammalian target of rapamycin inhibitor dyslipidemia in kidney transplant recipients. *Am J Transplant*. 2008;8(7):1384–1392.
29. Wan M, et al. Postprandial hepatic lipid metabolism requires signaling through Akt2 independent of the transcription factors FoxA2, FoxO1, and SREBP1c. *Cell Metab*. 2011;14(4):516–527.
30. Peterson TR, et al. mTOR complex 1 regulates lipin 1 localization to control the SREBP pathway. *Cell*. 2011;146(3):408–420.
31. Yecies JL, et al. Akt stimulates hepatic SREBP1c and lipogenesis through parallel mTORC1-dependent and independent pathways. *Cell Metab*. 2011;14(1):21–32.
32. Kapahi P, et al. With TOR, less is more: a key role for the conserved nutrient-sensing TOR pathway in aging. *Cell Metab*. 2010;11(6):453–465.
33. Seidah NG, et al. The secretory proprotein convertase neural apoptosis-regulated convertase 1 (NARC-1): liver regeneration and neuronal differentiation. *Proc Natl Acad Sci U S A*. 2003;100(3):928–933.
34. Horton JD, et al. Combined analysis of oligonucleotide microarray data from transgenic and knockout mice identifies direct SREBP target genes. *Proc Natl Acad Sci U S A*. 2003;100(21):12027–12032.
35. Maxwell KN, Soccio RE, Duncan EM, Sehayek E, Breslow JL. Novel putative SREBP and LXR target genes identified by microarray analysis in liver of cholesterol-fed mice. *J Lipid Res*. 2003;44(11):2109–2119.
36. Cohen J, Pertsemlidis A, Kotowski IK, Graham R, Garcia CK, Hobbs HH. Low LDL cholesterol in individuals of African descent resulting from frequent nonsense mutations in PCSK9. *Nat Genet*. 2005; 37(2):161–165.
37. Cohen JC, Boerwinkle E, Mosley TH Jr, Hobbs HH. Sequence variations in PCSK9, low LDL, and protection against coronary heart disease. *N Engl J Med*. 2006;354(12):1264–1272.
38. Graham MJ, et al. Antisense inhibition of proprotein convertase subtilisin/kexin type 9 reduces serum LDL in hyperlipidemic mice. *J Lipid Res*. 2007;48(4):763–767.
39. Frank-Kamenetsky M, et al. Therapeutic RNAi targeting PCSK9 acutely lowers plasma cholesterol in rodents and LDL cholesterol in nonhuman primates. *Proc Natl Acad Sci U S A*. 2008;105(33):11915–11920.
40. Chan JC, et al. A proprotein convertase subtilisin/kexin type 9 neutralizing antibody reduces serum cholesterol in mice and nonhuman primates. *Proc Natl Acad Sci U S A*. 2009;106(24):9820–9825.
41. Sharpe LJ, Brown AJ. Rapamycin down-regulates LDL-receptor expression independently of SREBP-2.

Biochem Biophys Res Commun. 2008;373(4):670–674.
42. Podder H, et al. Pharmacokinetic interactions augment toxicities of sirolimus/cyclosporine combinations. *J Am Soc Nephrol*. 2001;12(5):1059–1071.
43. Trotter JF, et al. Dyslipidemia during sirolimus therapy in liver transplant recipients occurs with concomitant cyclosporine but not tacrolimus. *Liver Transpl*. 2001;7(5):401–408.
44. Mathis AS, Dave N, Knipp GT, Friedman GS. Drug–related dyslipidemia after renal transplantation. *Am J Health Syst Pharm*. 2004;61(6):565–585.
45. Paul LC. Chronic allograft nephropathy: an update. *Kidney Int*. 1999;56(3):783–793.
46. Mueller MA, Beutner F, Teupser D, Ceglarek U, Thiery J. Prevention of atherosclerosis by the mTOR inhibitor everolimus in LDLR$^{-/-}$ mice despite severe hypercholesterolemia. *Atherosclerosis*. 2008;198(1):39–48.
47. Ouimet M, Franklin V, Mak E, Liao X, Tabas I, Marcel YL. Autophagy regulates cholesterol efflux from macrophage foam cells via lysosomal acid lipase. *Cell Metab*. 2011;13(6):655–667.
48. Uhlmann EJ, et al. Astrocyte-specific TSC1 conditional knockout mice exhibit abnormal neuronal organization and seizures. *Ann Neurol*. 2002;52(3):285–296.